Reaction Kinetics and Morphological Changes of Reactive Polymer−Polymer Interface

Hwang Yong Kim, Unyong Jeong, and Jin Kon Kim*

Department of Chemical Engineering and Polymer Research Institute, Electric and Computer Engineering Divisions, Pohang University of Science and Technology, Pohang, Kyungbuk 790-784, Korea

Received October 31, 2002; Revised Manuscript Received January 2, 2003

ABSTRACT: The temporal change of complex viscosity (η^*) of two plates consisting of an end-functional monocarboxylated polystyrene (PS−mCOOH) and poly(methyl methacrylates) (PMMA) with various amounts of poly(methyl methacrylate-*ran*-glycidyl methacrylate) (PMMA−GMA) was measured by a rotational rheometer. There were three distinct stages for the change of η^* with time: (i) stage I, where η^* increased rapidly at short times and approached a steady value at later times; (ii) stage II, where η^* did not change; and (iii) stage III, where η^* increased slowly again and reached a final value. The apparent reaction kinetics obtained from the results in stage I was a first-order reaction. The change of the interfacial roughness between two plates with reaction time was investigated by transmission electron microscopy and atomic force microscopy after selective removal of unreacted PS−mCOOH layer. At long reaction times, the interface became pinched off, and then microemulsions (and micelles) were formed in the PMMA phase.

I. Introduction

Reactive blending of two or more immiscible polymers with in situ reactive compatibilizers has been extensively employed for developing new materials with desirable physical and mechanical properties.[1−7] Yet, even though the reaction kinetics and the development of the interfacial morphology during the reaction are important, only a few studies are available.[4−6,8−17]

Employing various functional groups, Macosko and co-workers[9] studied the reaction kinetics in a reactive blending system. Since a reactive polymer with fluorescent group was used, they could detect a small amount of block (or graft) copolymer.[10] On the basis of their analysis, the reaction was classified as a second-order rate equation.[8,9]

Reactive blends are usually prepared by using an internal mixer or an extruder, where there is complex flow combined by shear and elongational flows.[1,7] Thus, some research groups employ a planar geometry of two polymers: for instance, two layers of each polymer are joined.[10−17] In this situation, the initial interface is well-defined and very sharp. Because the effect of complex external flow on interfacial morphology is excluded, the interface morphology depends mainly upon reaction conditions (time, temperature, and the amount of reactive groups) as well as the viscoelastic properties of two polymers.

Fredrickson[18,19] and O'Shaughnessy and co-workers[20,21] studied theoretically the reaction at a planar interface between two polymers. They showed that with increasing reaction time the reaction becomes mean-field type at initial times. But as the interface becomes saturated with in situ formed copolymers, the reaction rate decreases markedly and the reaction becomes diffusion-controlled. Because of the saturation of the interface, the corrugated interface is not predicted.

On the other hand, the corrugated interface of reactive blends with planar interface was experimentally observed by using atomic force microscopy (AFM) and transmission electron microscopy (TEM).[12−15] Jiao et al.[12] observed, via AFM, that the planar interface between benzylamine end-functionalized deuterated polystyrene (d-PS−NH_2) and poly(styrene-*ran*-maleic anhydride) (PSMA) becomes very rough (the roughness with ∼50 nm) after reacting at 190 °C for 72 h. They determined the excess of the interface (z^*) measured by depth profile of d-PS across the film by using forward recoil spectrometry (FRES). Since the z^*/R_g, where R_g is the radius of gyration of the graft copolymer, is related to the reduction of interfacial tension through the self-consistent mean-field theory,[22] they concluded the corrugated interface was due to the negative interfacial tension. We also reported that the interface thickness between PS−GMA and poly(butylene terephalate) (PBT) becomes very large, and the interfacial tension measured by the Neumann triangle method becomes negative for a very rough interface.[23] A negative interfacial tension due to a very rough interface for reactive blends was also predicted by molecular dynamics simulation.[24] Inoue and co-workers[14,15] showed that a planar interface between polyamide 6 (PA6) and maleic anhydride-*graft*-polysulfone (PSU−MAH) becomes very roughened, but there is no micelle (or microemulsion) formation measured by TEM. On the other hand, for PA6/PSU−MAH blends prepared by a mini-max molder, where an external shear or elongational force is applied, micelles are formed depending upon shear rate and the type of graft (or block) copolymer.[25−27] Very recently, the possibility of microemulsion formation was suggested for a planar reactive polymer interface.[3,6]

Oyama and Inoue[16] and Oyama et al.[17] proposed pseudo-first-order kinetics for PA6/PSU−MAH blends with a planar interface by employing the assumption that reaction rate is proportional to the areal density change investigated by X-ray photoelectron spectroscopy (XPS). Since they assumed that this reaction is similar

* To whom correspondence should be addressed: e-mail jkkim@postech.ac.kr.

10.1021/ma0257907 CCC: $25.00 © 2003 American Chemical Society
Published on Web 02/08/2003

Table 1. Molecular Characteristics of Polymers Used in This Study

polymer	M_w	M_w/M_n	mol % of GMA in PMMA−GMA	no. of functional groups (f) per chain	η^* (Pa s) at $\omega = 0.1$ rad/s and 180 °C
PS−mCOOH	135 000	1.13		1	8×10^3
PMMA	118 100	1.47	0	0	2.4×10^5
PMMA−GMA	115 500	1.7	2.0	12.5	2.5×10^5
PE					4×10^4

to the kinetics of a gas/solid system in surface science, the reaction rate is dependent on the number of vacant sites available for the reaction at the interface. The first-order kinetics of reactive blends with a planar interface might be unexpected since the interface reaction is usually taken as second-order kinetics because of the reaction of two different reactive groups.

Recently, Bousmina and co-workers[28,29] reported that the interdiffusion coefficient between two polymer chains with a planar interface could be measured by monitoring changes of rheological properties under a small-amplitude oscillatory shear which does not affect the diffusion mechanism. Once the rheological properties are also related to the amount of in situ formed graft (or block) copolymers for a reactive blend, the reaction kinetics might be evaluated if one monitors temporal changes of rheological properties. This rheological method is, of course, much easier than more sophisticated methods such as forward recoil spectrometry (FRES) and XPS, even though the excess of interface is not determined quantitatively.

In this study, we introduce a rheological technique to evaluate the reaction kinetics of an end-functional monocarboxylated polystyrene (PS−mCOOH) and poly(methyl methacrylate-*ran*-glycidyl methacrylate) (PMMA−GMA). The reaction between the carboxylic acid in PS−mCOOH and the epoxy groups in PMMA−GMA occurs easily at higher temperatures,[30−34] giving the in situ graft copolymers of PMMA-*g*-PS. The interface roughness with reaction time was studied by AFM after selectively removing unreacted PS phases as well as TEM. Finally, we clearly demonstrated that even for a reactive blend without external flow fields generated by an internal mixer or extruder, microemulsions (and micelles) could be formed as a result of pinch-off after the excessive corrugation.

II. Experimental Section

2.1. Materials. An end-functionalized monocarboxylated polystyrene (PS−mCOOH) synthesized anionically was purchased from Aldrich Chemical Co., and a poly(methyl methacrylate-*ran*-glycidyl methacrylate) (PMMA−GMA) was prepared by free-radical polymerization.[33,34] PMMA−GMA has ~12.5 functional units per chains on the basis of number-average molecular weight. To control the amount of GMA in PMMA phase, we employed neat poly(methyl methacrylate) (PMMA) which was purchased from Aldrich Chemical Co. We selected the molecular weight of neat PMMA whose complex viscosity (η^*) is very similar to that of PMMA−GMA. But, the η^* of PS−mCOOH is 40 times lower than that of PMMA (or PMMA−GMA). Molecular characteristics of polymers used in this study are summarized in Table 1.

Two plates, one for PS−mCOOH and the other for the mixture consisting of PMMA and PMMA−GMA, were prepared by compression molding on silicone wafer at 160 °C and annealed 130 °C for 24 h. This method gave a very smooth surface of polymer plates, which is necessary for investigating the interface morphology. The thickness of each plate was 0.3 mm, and the diameter was 25 mm. This kind of sandwich geometry was already employed to study the diffusion coefficients for compatible polymer blends.[29,35−38]

2.2. Rheological Properties. As soon as two plates were put into a rheometer (Advanced Rheometrics Expansion System, Rheometrics Co.) at three different temperatures (180, 200, and 220 °C) under a nitrogen environment, the complex viscosity (η^*) was monitored with time. Here, time zero was defined as the time when the heating chamber of the rheometer was closed. It is noted that the lower viscosity material (PS−mCOOH) was placed at the top. But even though we reversed the position of the two polymer plates (namely, we put the higher viscosity polymer at the top), we obtained the same results. The strain amplitude (γ_0) and the angular frequency (ω) were 0.005 and 0.1 rad/s, respectively, which lies in the linear viscoelastic regime. All measurements were performed with a 200 FRTN1 transducer with a lower limit of 0.08 g cm.

After the specimens were reacted for a given time, we first removed two parallel plates, inside which the welded plates were located, from the rheometer by unscrewing joints and then quenching them in ice water. It should be mentioned, however, that during unscrewing the torque in the rheometer must be carefully monitored in order to avoid any damage to the torque transducer.

2.3. Atomic Force Microscopy. To investigate the interface between two plates, the unreacted PS−mCOOH was removed by selective solvent of cyclohexane at 40 °C for 35 h. The interface thickness (or root-mean-square roughness) was obtained by AFM (Digital Instrument). The cantilevers used for imaging were Ultralevers of high aspect ratio with a specified spring constant of 0.4 N/m.

2.4. Transmission Electron Microscopy. Even though AFM is very convenient for investigating the interface, the existence of microemulsions (and/or micelles), which might be formed during the reaction, cannot be detected. Thus, to investigate the interface directly, we employed TEM (JEOL 1200EX) operated at 120 kV after ultrathin sectioning (RMC MT7000). The specimens were stained by ruthenium tetraoxide (RuO_4) for 15 min. Because of selective staining of RuO_4, the PS phase appeared dark in TEM images.

III. Results and Discussion

The plots of complex viscosity (η^*) at 180 °C with time for PS−mCOOH/100% of PMMA−GMA blends are shown in Figure 1. The changes of the storage and loss moduli (G' and G'') with time are similar to η^* change. In Figure 1 are added those plots of immiscible blend of PS−mCOOH and polyethylene (PE) as well as PS−mCOOH/PMMA blend. The η^* for the PS−mCOOH/PE blend does not change with time, and η^* remains the same as lower η^* for neat PS−mCOOH. This is attributed to the fact that the stresses are easily transferred into a polymer plate with lower η^*, as reported by Qui and Bousmina.[29] For instance, the viscosity of polymer/polymer blend with sandwich type planar geometry is given by[40]

$$1/\eta_{eff}^* = \phi_1/\eta_1^* + \phi_2/\eta_2^* + f(\zeta) \qquad (1)$$

in which ϕ_i and η_i ($i = 1, 2$) are volume fraction and viscosity of component i, and $f(\zeta)$ is a complicated function of slip (ζ) of the interface. When there is no slip of the interface, $f(\zeta)$ becomes zero. We found that measured η_{eff}^* for the PS−mCOOH/PE blend is lower than the predicted value based on eq 1 without slip,

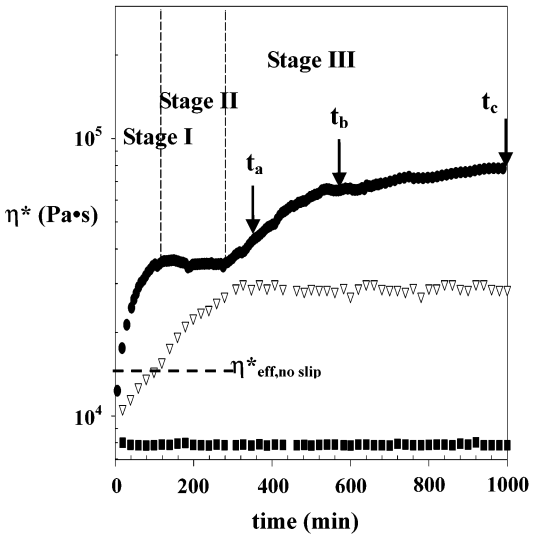

Figure 1. Plot of η^* at 180 °C vs time for PS−mCOOH/100% PMMA−GMA (●) as well as two nonreactive blend systems of PS−mCOOH/PMMA (▽) and PS−mCOOH/PE (■). Dashed line represents the average of viscosity (η^*_{eff}) of PS−mCOOH and PMMA (and PMMA−GMA) predicted by eq 1 with no slip condition.

indicating that interfacial slip could not be negligible in this blend system.

On the other hand, η^* for a blend of PS−mCOOH and neat PMMA slowly increased with welding time and reached a steady value at a considerably long time (∼6 h), after which η^* did not change any more. It should be noted that measured η^* at short welding times (less than 100 min) is lower than predicted η_{eff}^* based on eq 1 without slip, indicating that interfacial slip is important for short welding times. But, with increasing welding time, measured η^* is even higher than the predicted one without slip. These results are not expected, since PS−mCOOH/PMMA does not mix completely. However, the PS/PMMA blend shows a finite interfacial thickness (∼5 nm) due to small Flory's interaction parameter (χ).[39] Thus, as welding time (or contact time in the rheometer) goes on, two polymer chains can be mixed within this interfacial thickness, which causes η^* to increase. Interestingly, the interfacial morphology (or the root-mean-square (rms) of the roughness measured by AFM) changed with the welding time (or duration time). As shown in Figure 2, at the welding time of 6 h, the rms of interfacial roughness was increased to ∼5 nm from ∼2 nm at short welding times (<1 min). The roughness of ∼2 nm at short welding times is essentially the same as that prepared without using pressure applied by rheometer on the specimens. For PS−mCOOH/PE, interfacial slip resulting from a sharp interface, which is related to a large value of χ, should be considered; thus, η^* does not increase with welding time. Even though the welding process as well as diffusion of two plates with finite interfaces would be an interesting subject, we do not discuss in detail the phenomenon of nonreactive polymer blends.

For a reactive blend consisting of PS−mCOOH and 100% of PMMA−GMA, η^* increased within short times compared with nonreactive PS−mCOOH/PMMA blend (120 vs 340 min). Interestingly, η^* did not change at medium reaction times ($120 < t < 280$ min) and then slowly increased again to reach a steady value. This phenomenon was quite different from nonreactive PS−mCOOH/PMMA blend, where there was only a slow increase in η^* before reaching a steady value.

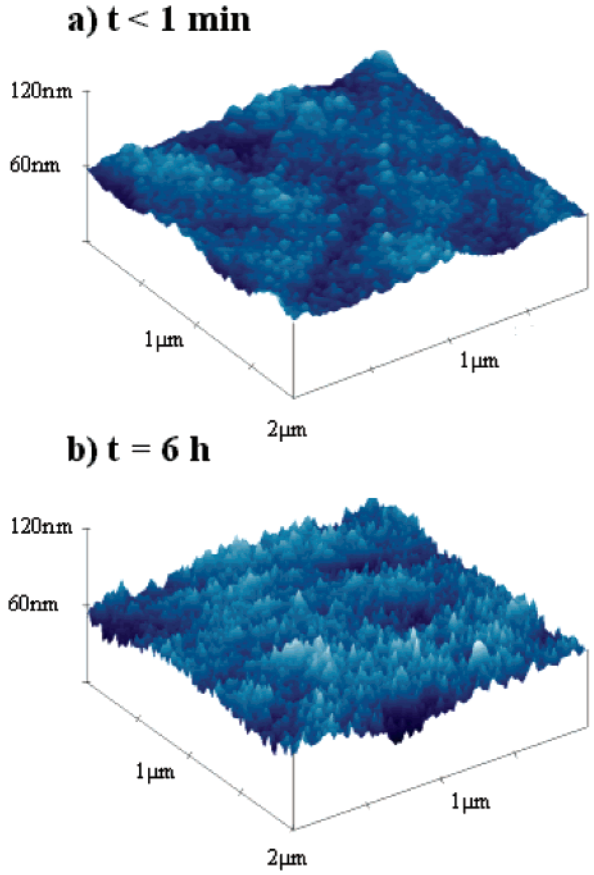

Figure 2. AFM images for PS−COOH/PMMA at 180 °C for two welding times (or contacting time in the rheometer). (a) A short welding time (less than 1 min). In this situation, as soon as two plates were in contact with each other at 180 °C in the rheometer, the sample was removed. (b) After 6 h welding. The values of rms roughness of two cases are 2 and 5 nm, respectively.

On the basis of results given in Figure 1, we divided the reactive blend into three different stages: stage I, before reaching the first plateau value of η^*; stage II, where η^* does not change with reaction time; and stage III, where η^* is again increased before reaching a final value.

3.1. Stage I. Because of the increase of interface adhesion strength due to the coupling reaction between carboxylic acid and epoxy groups, η^* increased rapidly with reaction time. The plots of η^* at 180 °C vs reaction time for blends with various amounts of PMMA−GMA are shown in Figure 3. In Figure 4 are given AFM images for a blend consisting of PS−mCOOH and 10/90 wt/wt PMMA−GMA/PMMA reacted for three reaction times (t_1, t_2, and t_3; marked by the arrows in Figure 3). We found that the AFM image of a specimen taken at the center of the plate is essentially the same as that taken at the rim of the plate, indicating that a small oscillatory shearing force does not affect interfacial morphologies of reactive blends. In Figure 3 the initial slopes and plateau values of η^* at stage I were almost the same regardless of PMMA−GMA contents, which suggests that during stage I most reactions occurred between two functional groups existing near the interface. However, the time to reach the plateau value η^* for a blend with 10% PMMA−GMA was longer than that of other two blends (20 and 100% PMMA−GMA).

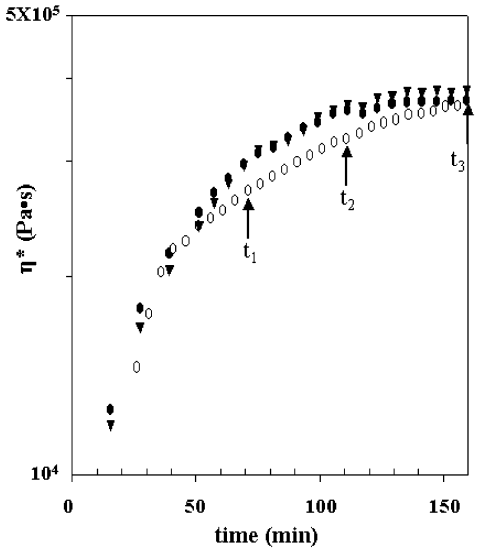

Figure 3. Plots of η^* at 180 °C vs time for PS-mCOOH/PMMA with various amounts of PMMA−GMA: (○) 10, (▼) 20, and (●) 100 wt % PMMA−GMA.

Because of a slow approach to plateau value of η^* for the 10 wt % of PMMA−GMA compared with other two blends, we employed this blend to correlate the change of η^* with the conversion $[X(t)]$ of the in situ formed copolymers as follows:

$$X_A(t) = [\eta^*(t) - \eta^*_{no}(t)]/[\eta^*_{sat} - \eta^*_{no,sat}] \qquad (2)$$

where η^*_{sat} is the plateau value of η^* of reactive blend at stage I, whereas the subscript "no" in η^* represents the PS−mCOOH/PMMA blend without PMMA−GMA, which are obtained from Figure 1.

Now, we applied two kinds of simple reaction rate equations (the first and the second-order kinetics)

$$-\ln(1 - X_A) = k_1 t \qquad (3)$$

for the first-order reaction kinetics and

$$\ln[(M - X_A)/M(1 - X_A)]/[C_{B0}(M - 1)] = k_2 t \quad \text{for } M \neq 1 \qquad (4a)$$

$$X_A/[C_{B0}(1 - X_A)] = k_2 t \quad \text{for } M = 1 \qquad (4b)$$

for the second-order reaction kinetics. Here, k_1 and k_2 are the reaction constants, and $M = C_{B0}/C_{A0}$ in which C_{A0} and C_{B0} are initial concentrations of reactive groups COOH and GMA, respectively.

In the blend consisting of PS−mCOOH/PMMA with 10 wt % PMMA−GMA, the concentrations of GMA and COOH functional groups are not much different. This is because a PMMA−GMA chain has ∼12.5 GMA functional groups. Therefore, this reaction should not be classified as a pseudo-first-order reaction due to the excessive amount of one functional group. Once the concentration of one reactant group (GMA) is much greater than that of COOH, which is the case of PS−mCOOH and 20 and 100% PMMA−GMA, the left term in eq 4a becomes the same as that in eq 3.

Figure 5 gives plots of conversion vs reaction time based on the first-order reaction kinetics given by eq 3 (left panel) and the second-order reaction kinetics given by eq 4a (right panel) for a blend of PS−mCOOH and 10 wt % PMMA−GMA reacted at three different tem-

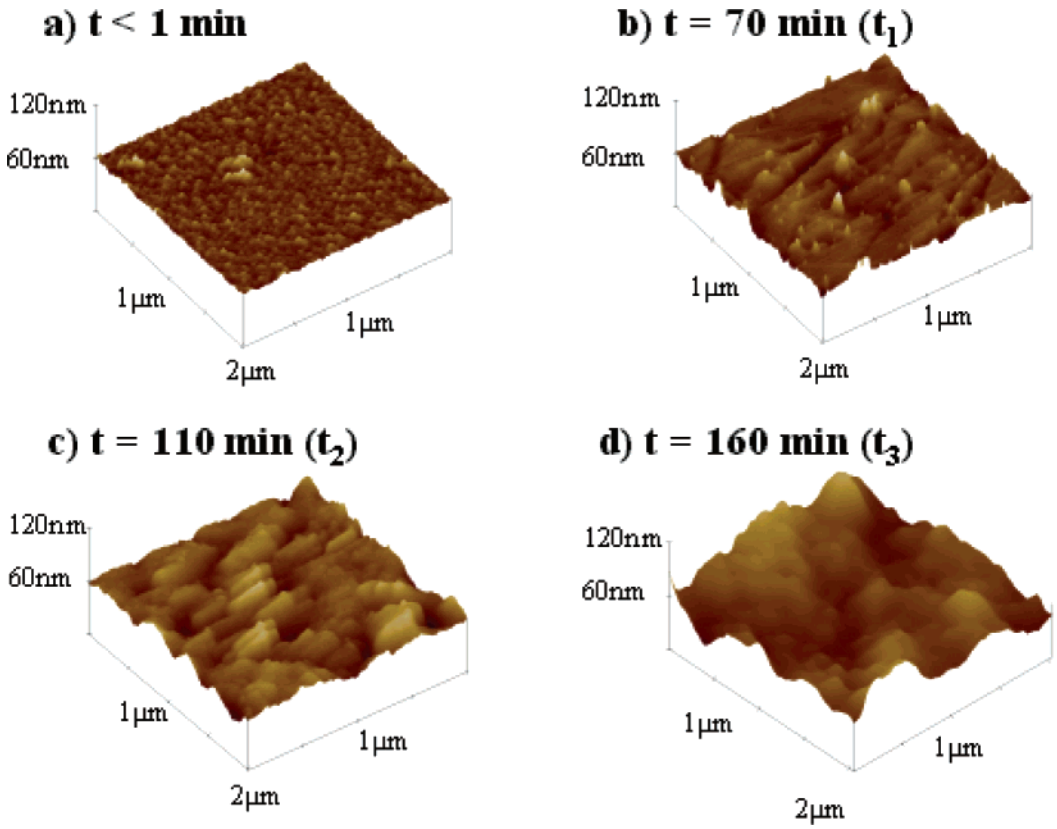

Figure 4. AFM images (2 μm × 2 μm) for specimens reacted at 180 °C for three reaction times (t_1, t_2, and t_3 as shown in Figure 3) as well as for a short contact time (less than 1 min) in the rheometer for PS−mCOOH/(10/90 wt/wt PMMA−GMA/PMMA). (a) t < 1 min; (b) $t = t_1 = 70$ min; (c) $t = t_2 = 110$ min; and (d) $t = t_3 = 160$ min. The values of rms roughness at reaction times (a)−(d) are 2, 5, 8, and 39 nm, respectively.

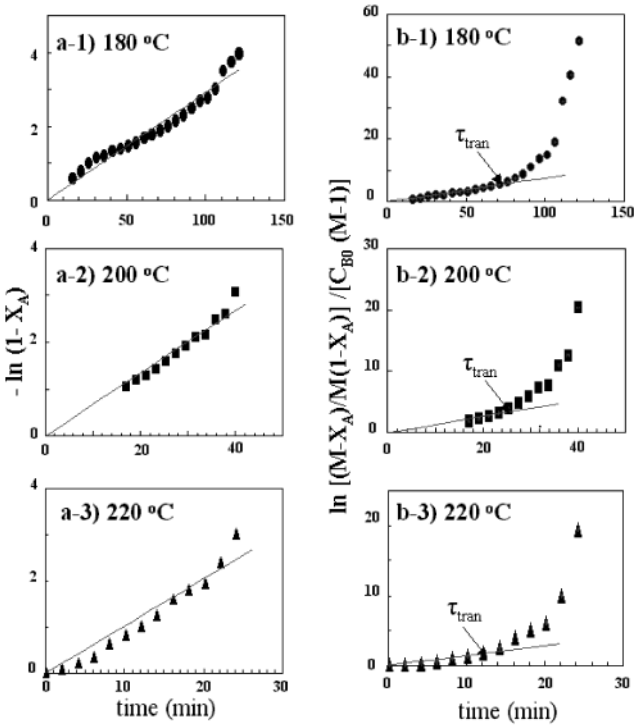

Figure 5. Plots of conversion vs reaction time based on the first-order reaction kinetics given by eq 3 (left panel) and the second-order reaction kinetics given by eq 4a (right panel) for PS−mCOOH/(10/90 wt/wt PMMA−GMA/PMMA) ((●) 180, (■) 200, and (▲) 220 °C). Also, shown in the right panel is a transition reaction time (τ_{tran}) before which experimental data are well fitted with the second-order reaction kinetics.

peratures. Here, the conversion $X_A(t)$ for both cases was estimated by eq 1. The overall reaction kinetics at three temperatures is well described by the first-order reaction kinetics compared with second-order reaction kinetics when the entire range of the reaction time corresponding to stage I is considered. However, the experimental data can also be well fitted with the second-order reaction kinetics at short times less than a transition reaction time (τ_{tran}), and this decreased with increasing reaction temperature. Here, τ_{tran} is the reaction time after which the second-order reaction (eq 4a) cannot fit experimental data any more. From the Arrhenius plot (the reaction constant vs inverse temperature), we obtained the activation energy (ΔE) of 57 kJ/mol on the basis of the first-order reaction, which is consistent with the reported value (84 kJ/mol) of the PS−COOH/PMMA−GMA blend.[8] We found that, regardless of the amounts of PMMA−GMA in the blend, k_1 (thus ΔE) is almost the same. For instance, k_1 at 180 °C for blends with 10, 20, and 100% PMMA−GMA is 0.029, 0.024, and 0.028 min^{-1}, respectively. In the meantime, ΔE for a blend with 10 wt % PS−GMA was calculated to be 217 kJ/mol when the second-order reaction was used at $t < \tau_{tran}$.

On the basis of the above results, we concluded that the overall reaction between PS−mCOOH and PMMA−GMA plates at stage I was described by first-order reaction kinetics. Since the reaction might also be described by the second-order reaction at $t < \tau_{tran}$, we consider that the interfacial morphology can change much at $t = \tau_{tran}$. This is confirmed by the AFM image, as shown in Figure 4, that the root-mean-square (rms) roughness of the interface was less than 5 nm before τ_{tran} (∼70 min at 180 °C). However, the rms of the

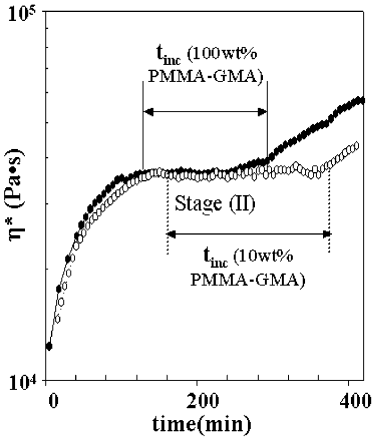

Figure 6. Plot of η^* at 180 °C vs reaction time for PS−mCOOH/PMMA with two different amounts of PMMA−GMA ((○) 10%; (●) 100%). There exists an incubation period (t_{inc}) where η^* did not increase with time, and t_{inc} decreased with increasing the amount of PMMA−GMA.

interface was increased up to ∼40 nm at the end of stage I ($t \sim 160$ min). Thus, we assumed that τ_{tran} corresponds to the reaction time after which the interface was almost covered by monolayer of in situ formed graft (or block) copolymer. The radius of gyration of PMMA-*g*-PS formed in situ from PS−mCOOH and PMMA−GMA blend was calculated to be ∼15 nm on the basis of M_n. Once the interface is almost covered with graft (or block) copolymer, the overall reaction depends only upon the vacant site, as suggested by Inoue and co-workers.[16,17] It is noted from Figures 3−5 in ref 16 that the second-order reaction kinetics predicted well the experimental data at shorter times, whereas the experimental data for entire reaction times were well fitted by the first-order reaction kinetics. Also, one can see in Figure 4 of ref 16 that the τ_{tran} decreased with increasing temperature, which is consistent with our experiment.

These results suggest that the diffusion-controlled reaction regime predicted by O'Shaughnessy and co-workers[20,21] as well as Fredrickson[18,19] can occur when the reaction time is larger than τ_{tran}. This phenomenon was also found for the silicone oxide growth mechanism on the silicone substrate (gas−solid reaction).[41] For shorter times, the growth mechanism is reaction-controlled, but it becomes diffusion-controlled at longer times. Finally, even after $t > \tau_{tran}$ the rms values still increased due to more reactions, which causes interface roughness. In this situation, the flat interface does not keep any more due to accommodating a larger amount of graft copolymers. When plotting the conversion against time, we observed that the slope was ∼1 at shorter times, then became ∼0.5 at intermediate times, and finally became very small at longer reaction times. This is consistent with the prediction by O'Shaughnessy and co-workers[20,21] as well as Fredrickson.[18,19]

3.2. Stage II. As the interface was densely packed by in situ formed graft copolymers, or the thickness of the interface is several times larger than the radius of gyration of graft copolymer, further reaction only occurs after each chain penetrates into these layers. Figure 6 gives a plot of η^* at 180 °C vs reaction time for PS−mCOOH/PMMA with two different amounts of PMMA−GMA. There exists an incubation period (t_{inc}) where η^* did not increase with time. During this period, small amounts of reactive chains might react near the interface, but these do not contribute to any detectable

change in interface roughness and thus rheological properties. It is seen in Figure 6 that t_{inc} decreased with increasing the amount of PMMA−GMA (3.5 h for a blend with 10% PMMA−GMA vs 2.7 h for another blend with 100% PMMA−GMA). This is because the larger the concentration of reactive groups in bulk, the easier further reaction occurs. We also observed that the rms measured by AFM remained almost the same (∼40 nm) during t_{inc}.

Since the penetration rate of PMMA−GMA and PS−mCOOH chains can be related to the diffusion through the graft copolymer layer, we first estimate the self-diffusion coefficient (D_0) of PMMA and PS. From reported self-diffusion coefficients of PS[42] and PMMA,[43] the values of D_0 at 180 °C of PS−mCOOH and PMMA−GMA employed in this study are ∼30 and ∼0.6 nm²/s, respectively. Here, we assumed that D_0 of PS−mCOOH and PMMA−GMA are the same as those of PS and PMMA once the viscosities of PMMA−GMA and PS−mCOOH are the same as neat PMMA and PS. With these two values, the penetration distances ($\sqrt{D_0 t}$) of PS−mCOOH and PMMA−GMA chains into their own chains during 2.7 h (stage II) are ∼550 and 75 nm, respectively. But, we found via AFM that the interfacial thickness during stage II is ∼40 nm, which indicated that the incubation time for the stage II seemed to be longer than expected. However, the above values are obtained from self-diffusion coefficients. Once PMMA−GMA (or PS−mCOOH) chains penetrate through the in situ formed copolymer layer, the trace diffusion coefficient is much slower than the self-diffusion coefficient. Green et al.[43] showed that the diffusion of neat PMMA into PS−PMMA block copolymer matrix, whose constituent block molecules are the same as neat PMMA and the microdomains are lamellar, was 10 times slower than that into neat PMMA matrix. Although in situ formed copolymer would be graft type rather than block type for this blend system, we still consider that the diffusion of PMMA−GMA into graft copolymer layer would be much more retarded than that into neat PMMA−GMA, which can explain the results given in Figure 6. Therefore, we concluded that after the initial reaction the incubation time for further reaction might exist mainly due to slow diffusion of PMMA−GMA chains. This is complemented by the fact that for PS−mCOOH/100% PMMA−GMA the ratio of t_{inc} at 200 °C to that at 180 °C was 0.18 (i.e., 0.5 h vs 2.7 h). Once the penetration distance is assumed to be the same for both cases, t_{inc} is simply inversely proportional to D. Because of $D \sim 1/\eta$, $t_{inc} \sim \eta$. Interestingly, for PMMA−GMA with higher viscosity compared with PS−mCOOH, η at 200 °C is 5 times lower than that at 180 °C.

3.3. Stage III. When each polymer chain penetrates into the brushlike layer of graft (or block) copolymers, additional reactions can proceed. To reduce the incubation time that occurred in stage II, we employed 100% PMMA−GMA. We found from Figure 1 that η^* increased steadily with time before attaining a final value, although the increase in η^* with time (or slope in Figure 1) during stage III was much reduced compared with that during stage I. The difference in slopes during stages I and III might be due to the fact that reaction near the interface controlled the amount of graft copolymer during stage I, whereas the effect of the diffusion becomes important in addition to the reaction during stage III.

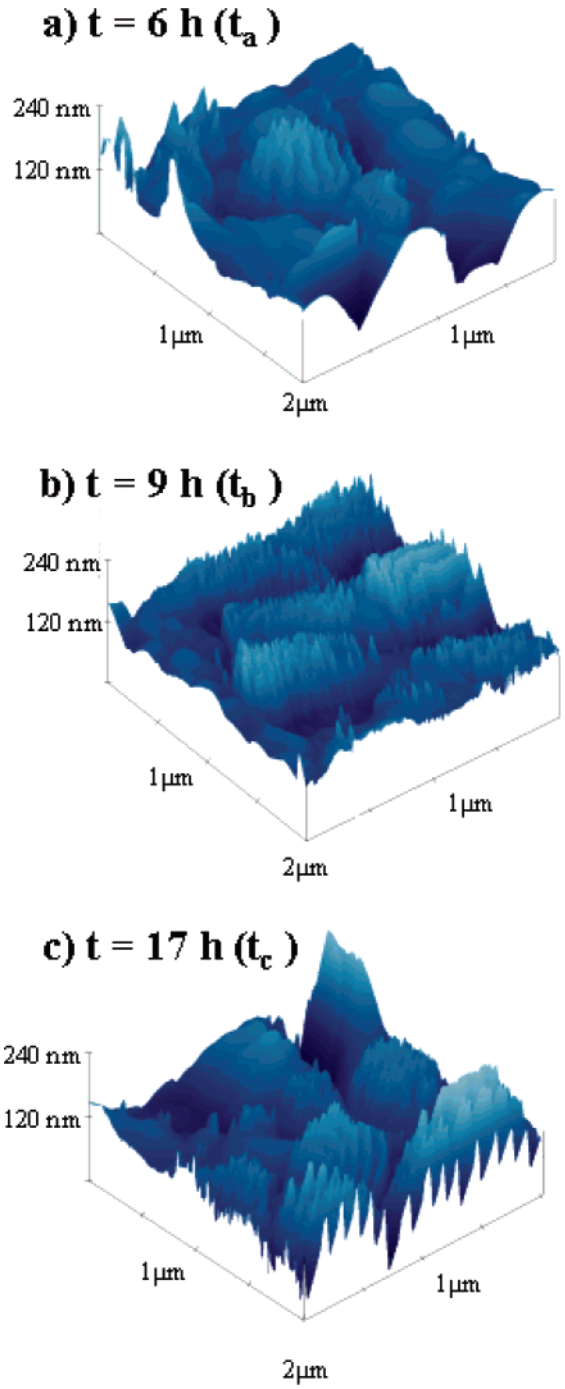

Figure 7. AFM images (2 μm × 2 μm) of PS−mCOOH/100 wt % PMMA−GMA reacted at 180 °C for three reaction times (t_a, t_b, and t_c) as shown in Figure 1: (a) $t = t_a = 6$ h; (b) $t = t_b = 9$ h; (c) $t = t_c = 17$ h. The values of rms roughness at reaction times (a)−(c) are 96, 160, and 180 nm, respectively.

As more graft chains accumulate in the interface, the roughness of the interface increases. AFM images for the interface at three reaction times (t_a, t_b, and t_c in Figure 1) during stage III are given in Figure 7. With increasing reaction time, the rms roughness increased steadily, which suggests that the increase in η^* at stage III is correlated with increased interface thickness due to the continuing reaction. The large roughened interface similar to Figure 8 was observed for reactive layers previously.[5,6,13]

Although changes in the interfacial morphologies with reaction time were clearly seen in AFM images, as shown in Figure 7, we cannot know whether micro-

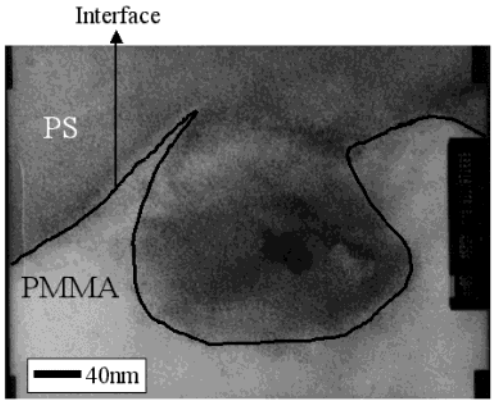

Figure 8. TEM image of PS−mCOOH/100 wt % PMMA−GMA reacted at 180 °C for 6 h reaction, which corresponds to beginning of stage III. Pinch-off was clearly observed. However, no microemulsion (or micelle) was observed during this time.

emulsions (and/or micelles) consisting of graft copolymer formed in situ exist in one of the phases. To the best of our knowledge, there has been no report on microemulsion (and/or micelles) formation when two films or plates consisting of reactive groups are reacted without external force, although a significant roughness of the interface has been reported.[12−15] In the meantime, when a reactive blend is prepared by a mixer where a strong shear (or elongational) flow is applied, micelles are formed in the matrix depending very much on molecular structures of in situ formed graft (or block) copolymer as well as the amount of reactive groups.[25−27] For instance, when a Y-shaped type of graft copolymer is formed during the reaction, these graft copolymers can be easily pulled off from the interface toward the upper phase. Microemulsions could not be detected by AFM since these microemulsions were also wiped out together with one of these phases; thus, only TEM images are needed to verify the microemulsion (and/or micelles) formation. The difference between microemulsions and micelles is mainly due to the size. For instance, the micelles contain only PS block (or graft) inside the matrix of PMMA homopolymer. Thus, the size of micelles is similar to 2 times the radius of gyration of PS block (or graft), which would be ∼18 nm. But, the microemulsions contain both PS homopolymer and PS graft (or block) chains; thus, the size (∼100 nm) should be larger than that of micelles.

To form a microemulsion during the reaction without any external force, the interface should be first pinched off and then encapsulated by one of the components. Or, fast-diffusing species (PS chains) could be diffused through the barrier consisting of graft copolymer layer and reacted with a GMA group in the PMMA−GMMA phase. It is less likely that PMMA−GMA chains diffused through this barrier and reacted with a COOH group in the PS−mCOOH phase because their diffusion coefficients are much less than that of PS−mCOOH. Figure 8 gives the TEM image at the beginning of stage III, where the pinch-offs of in situ formed graft (or block) copolymer are clearly observed from a very rough interface. However, microemulsions (or micelles) were not observed until the reaction time of 6 h.

On the other hand, with further reaction (for instance, the reaction time of 17 h), microemulsions with size of ∼100 nm (solid circles) as well as micelles with size of 10−20 nm (dashed circles) exist in the PMMA phase, as shown in Figure 9. From Figure 9, the rms of

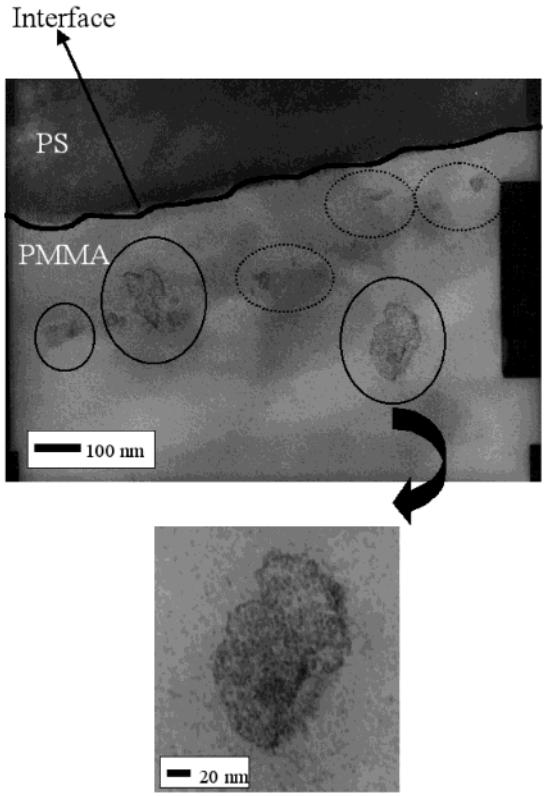

Figure 9. TEM image of PS−mCOOH/100 wt % PMMA−GMA reacted at 180 °C for 17 h reaction, which corresponds to final of stage III. Both microemulsions inside solid circles and micelles inside dashed circles are clearly seen.

roughness (∼30 nm) at regions where microemulsions are seen was much smaller than that (∼180 nm) measured by AFM images (see Figure 7c). This is because rms of roughness measured by AFM is the average value of roughness. Namely, at a reaction time of 17 h, many regions remained pinched-offs similar to those seen in Figure 8, which contributed large values of rms roughness. We also found in Figure 9 that microemulsions (or micelles) were not observed in the PS phase. One of the reasons might be attributed to the fact that the shape of in situ formed graft copolymers might become an inverted Y-shape, and PMMA chains consists of two branches of the Y-shape. This is because only 1−2 PS chains were grafted to PMMA−GMA chains, even though PMMA−GMA has many functional units (∼12.5) of GMA across the main chain.[33] Once one considers the steric hindrance between graft copolymers, PS chains belonging to one branch of Y-shape should be located inside the interface curvature to fill more graft chains at the interface. Thus, PMMA chains can encapsulate PS chains with increasing corrugation (or curvature) of the interface.

It might be argued that a very small oscillatory force ($\omega = 0.1$ rad/s and $\gamma_0 = 0.005$) accelerates the microemulsion formation. However, even though a simple welding experiment was done for 17 h without oscillatory force, these microemulsions were also found in the PS−mCOOH/PMMA−GMA blend. Another possibility of microemulsion formation in the PMMA phase is due to the much viscose PMMA−GMA and thus a very slow diffusion compared with that of PS−mCOOH. Thus, it is interesting to investigate this possibility by using another blend with PS−mCOOH and lower molecular weight of PMMA−GMA.

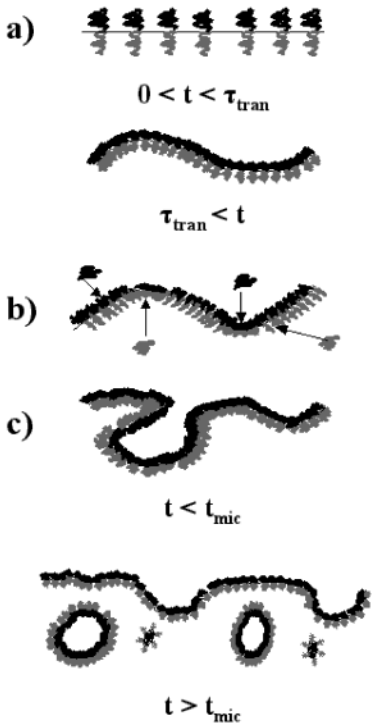

Figure 10. Interfacial morphology change of a reactive blend with reaction time. (a) Stage I, where in situ reaction occurs near the interface at $t < \tau_{tran}$, and in situ formed graft copolymers are formed at least a single layer at $t > \tau_{tran}$. (b) Stage II, where the interface thickness does not change, but reactant groups diffuse into the brush layer. (c) Stage III, where pinch-offs are observed at the beginning of this stage, and then microemulsions and micelles are formed at very long reaction times ($t > t_{mic}$).

The fact that microemulsions (or micelles) formation without shear (or elongational flow) has not been reported might be due to short reaction times,[12−15] or the interfacial tension between two polymers studied previously[12,14,15] might be very large compared with a small one for the PS/PMMA blend. Note that we observed the microemulsions for PS−mCOOH/100% of PMMA−GMA reacted at 180 °C for 17 h. This suggests that, in order to see microemulsions formed in the planar interface, the reaction time would be very large or the molecular weights of two plates are much reduced. The existence of microemulsion near the reactive interface between amine-terminated PS and maleic anhydride-terminated PMMA was indeed suggested very recently even when the reaction time was short (∼1 h at 200 °C), once molecular weights of both components are less than 20 kg/mol.[6]

IV. Conclusion

In this study, we proposed a rheological method to observe the reaction kinetics in the reactive blending system and correlated morphological change at the interface with rheological properties. According to rheological results as well as interfacial morphological changes measured by AFM and TEM, three distinct stages can be considered for reactive blends with planar geometry.

In stage I, a coupling reaction starts, and the copolymers formed by in situ reaction cover the interface. Because of the increase of interface adhesion by this reaction, the modulus increases. During very short reaction time until the interface is not roughened, the reaction is also characterized by the second-order reaction in addition to the first-order reaction. However, as the reaction continues ($t > t_{tran}$), the interface becomes saturated and then corrugated. During this time interval, the first order is suitable to analyze the kinetics.

In stage II, the reactive chains near the interface are totally consumed. Thus, chains should move through the brushlike graft copolymer layer. We found that η^* does not change with reaction time during the second stage, which suggests that incubation time exists. This incubation time was longer than the value calculated by the self-diffusion coefficient because the diffusion of homopolymer through the copolymer is slower than the self-diffusion.

In stage III, since chains can diffuse through the brushlike layer, the reaction can occur again. The interface is more corrugated and becomes large; thus, η^* increased again. When the corrugation of interface was enough (or $t > t_{mic}$), the copolymer began to pinch-off, which finally became microemulsions (and micelles). Changes of interfacial morphologies during the reaction are schematically drawn in Figure 10.

Acknowledgment. We thank Profs. C. W. Macosko and T. Ougizawa for critical reading of this manuscript and several comments. This work was supported by National Research Laboratory program by MOST and Applied Rheology Center governed by KOSEF.

References and Notes

(1) Ide, F.; Hasegawa, A. *J. Appl. Polym. Sci.* **1974**, *18*, 963.
(2) Pagnoulle, C.; Korning, C.; Leemans, L.; Jérôme, R. *Macromolecules* **2000**, *33*, 6275.
(3) Koulic, C.; Yin, Z.; Pagnoulle, C.; Gilbert, B.; Jérôme, R. *Polymer* **2001**, *42*, 2947.
(4) Pagnoulle, C.; Jérôme, R. *Macromolecules* **2001**, *34*, 965; *Polymer* **2001**, *42*, 1893.
(5) Yin, Z.; Koulic, C.; Pagnoulle, C.; Jérôme, R. *Macromol. Chem. Phys.* **2002**, *203*, 2021.
(6) Yin, Z.; Koulic, C.; Pagnoulle, C.; Jérôme, R. *Langmuir* **2003**, *19*, 453.
(7) *Reactive Extrusion: Principles and Practice*; Xanthos, M., Ed.; Hanser: New York, 1992; Chapter 4.
(8) Guégan, P.; Macosko, C. W.; Ishizone, T.; Hirao, A.; Nakahama, S. *Macromolecules* **1994**, *27*, 4993.
(9) Orr, C. A.; Cernohous, J. J.; Guegan, P.; Hirao, A.; Jeon, H. K.; Macosko, C. W. *Polymer* **2001**, *42*, 8171.
(10) Schulze, J. S.; Moon, B.; Lodge, T. P.; Macosko, C. W. *Macromolecules* **2001**, *34*, 200.
(11) Schulze, J. S.; Cernohous, J. J.; Hirao, A.; Lodge, T. P.; Macosko, C. W. *Macromolecules* **2000**, *33*, 1191.
(12) Jiao, J.; Kramer, E. J.; de Vos, S.; Möller, M.; Koning, C. *Polymer* **1999**, *40*, 3585; *Macromolecules* **1999**, *32*, 6261.
(13) Lyu, S. P.; Cernohous, J. J.; Bates, F. S.; Macosko, C. W. *Macromolecules* **1999**, *32*, 106.
(14) Koriyama, H.; Oyama, H. T.; Ougizawa, T.; Inoue, T.; Weber, M.; Koch, E. *Polymer* **1999**, *40*, 6381.
(15) Kuroda, T.; Torikai, K.; Oyama, H. T.; Ougizawa, T.; Inoue, T.; Weber, M. *Kobunshi Ronbunshu* **1999**, *56*, 860.
(16) Oyama, H. T.; Inoue, T. *Macromolecules* **2001**, *34*, 3331.
(17) Oyama, H. T.; Ougizawa, T.; Inoue, T.; Weber, M.; Tamaru, K. *Macromolcules* **2001**, *34*, 7017.
(18) Fredrickson, G. H. *Phys. Rev. Lett.* **1996**, *76*, 3440.
(19) Fredrickson, G. H.; Milner, S. T. *Macromolecules* **1996**, *29*, 7386.
(20) O'Shaughnessy, B.; Sawhney, U. *Macromolecules* **1996**, *29*, 7230.
(21) O'Shaughnessy, B.; Vavylonis, D. *Macromolecules* **1999**, *32*, 1785; *Europhys. Lett.* **1999**, *45*, 638.
(22) Shull, K. R.; Kramer, E. J. *Macromolecules* **1990**, *23*, 4769.
(23) Kim, J. K.; Jeong, W. Y.; Son, J. M.; Jeon, H. K. *Macromolecules* **2000**, *33*, 9161.
(24) Yeung, C.; Herrmann, K. A. *Macromolecules* **2003**, *36*, 229.
(25) Charoensirisomboon, P.; Chiba, T.; Solomko, S. I.; Inoue, T.; Weber, M. *Polymer* **1999**, *40*, 6803.

(26) Charoensirisomboon, P.; Inoue, T.; Weber, M. *Polymer* **2000**, *41*, 6907, 4483.
(27) Pan, L.; Chiba, T.; Inoue, T. *Polymer* **2001**, *42*, 8825.
(28) Bousmina, M.; Qiu, H.; Grmela, M.; Klemberg-Sapieha, J. E. *Macromolecules* **1998**, *31*, 8273.
(29) Qiu, H.; Bousmina, M. *Macromolecules* **2000**, *33*, 6588.
(30) Kim, J. K.; Lee, H. *Polymer* **1996**, *37*, 305.
(31) Jeon, H. K.; Kim, J. K. *Macromolecules* **1998**, *31*, 9273.
(32) Jeon, H. K.; Kim, J. K. *Polymer* **1998**, *39*, 6227; *Korean Polym. J.* **1999**, *7*, 124.
(33) Jeon, H. K.; O., H. T.; Kim, J. K. *Polymer* **2001**, *42*, 3259.
(34) Jeon, H. K.; Kim, J. K. *Macromolecules* **2000**, *33*, 8200.
(35) Qiu, H.; Bousmina, M. *J. Rheol.* **1999**, *43*, 551.
(36) Qiu, H.; Bousmina, M.; Dealy, J. M. *Rheol. Acta* **2002**, *41*, 87.
(37) Vaudreuil, S.; Qiu, H.; Kaliaguine, S.; Grmela, M.; Bousmina, M. *Macromol. Symp.* **2000**, *158*, 155.
(38) Ernst, B.; Koenig, J.; Muller, R. *Macromol. Symp.* **2000**, *158*, 43.
(39) Russell, T. P.; Menelle, A.; Hamilton, W. A.; Smith, G. S.; Satija, S. K.; Majkrzak, C. F. *Macromolecules* **1991**, *24*, 5721.
(40) Bousmina, M.; Palierne, J. F. *Utracki, L. A. Polym. Eng. Sci.* **1999**, *39*, 1049.
(41) Sze, S. M., Ed.; *VSLI Technology*; McGraw-Hill: New York, 1983; pp 132−140.
(42) Green, P. F.; Kramer, E. J. *Macromolecules* **1986**, *16*, 1108.
(43) Green, P. F.; Russell, T. P.; Jérôme, R.; Granville, M. *Macromolecules* **1988**, *21*, 3266.

MA0257907